Diurnal Yarkovsky effect as a source of mobility of meter-sized asteroidal fragments

II. Non-sphericity effects

David Vokrouhlický

Institute of Astronomy, Charles University, V Holešovičkách 2, CZ-180 00 Prague 8, Czech Republic (vokrouhl@mbox.cesnet.cz)

Abstract. The diurnal Yarkovsky effect, a perturbing force on meter-sized orbiting bodies caused by anisotropic heating and emission of thermal radiation from small spinning solar system bodies, is computed for spheroidal-shaped bodies with an arbitrary flattening. The solution is derived in analytical form for a body which rotates around its axis of symmetry. A numerical solution is presented for the more general case of a precessing body, where the symmetry axis tumbles around a fixed angular momentum vector. In both cases, the obtained Yarkovsky force is compared with the corresponding thermal force acting on a spherical body of the same mass. Differences of up to a factor of 3 are found, depending on the geometric parameters of the body and its rotational state. However, the agreement between the derived force values in the two cases is much better when an average over all possible pole orientations of a tumbling spheroidal body and the solar position over its revolution around the Sun is considered. This result suggests that the simplified formulation of the diurnal Yarkovsky force based on a spherical geometry can be used, without introducing major mistakes, for long-term integrations of the orbits of small asteroidal fragments in the Solar System.

Key words: celestial mechanics, stellar dynamics – minor planets, asteroids

1. Introduction

Thermal forces due to anisotropic heating and re-emission of thermal radiation from small, spinning Solar System bodies (usually called "Yarkovsky effects") have been recently found to provide an efficient transport mechanism for meter-sized asteroidal fragments into resonant channels which deliver them to the near-Earth space (Farinella et al. 1998, Hartmann et al. 1998). Although so far most models for these effects have assumed spherically shaped bodies, real asteroidal fragments probably have very irregular shapes. There are several arguments for this conclusion: (i) fragments from asteroidal catastrophic collisions probably have shapes similar to fragments obtained in laboratory hypervelocity impact experiments, which typically show approximatelly 2 : 1 ratio between the longest and shortest axes

(Fujiwara et al. 1978, 1989; Catullo et al. 1984; Giblin et al. 1994); (ii) asteroid lightcurve photometry, radar observations and spacecraft reconnaissance, all show that asteroids in the size range between ≈ 1 km and a few hundred km have irregular fragment-like shapes (see e.g. Binzel et al. 1989, Ostro et al. 1995; Zappalà & Farinella 1997); (iii) meteorites recovered on the ground have irregular shapes, including the largest ones (a few m across), such as Hoba and Willamette. Note that the size range for which these data are relevant (from ≈ 1 cm to > 1 km) brackets the size range for which Yarkovsky effects are significant (from about 0.1 to 100 m, see Farinella et al. 1998).

All of this casts doubt on the current thermal models from which Yarkovsky effects are estimated, as they are based on questionable simplifying assumptions as far as the shape of the body is concerned. Actually, complete models including thermal conduction across the body have been developed only for spheres (Vokrouhlický 1998 - hereafter also called paper I; see also Afonso et al. 1995 and Rubincam 1998). The reason is that the view has prevailed that a generalization for different shapes would require a much more involved mathematical technique and the results would be algebraically very complicated.

Luckily, there is an important circumstance which helps reducing the complexity of models for the diurnal Yarkovsky effect. In most relevant situations the thermal penetration depth, characterizing approximately the thickness of the surface layer undergoing temperature variations due to external heating, is very small. For instance, thermal parameters appropriate for a non-porous basalt surface would correspond to a thermal penetration depth of about $0.4\sqrt{P}$ mm (here P is the spin period of the body in seconds), whereas an insulating regolith cover would further decrease this figure (Farinella et al. 1998, Hartmann et al. 1998). This implies that the thermal conduction across the body is extremely weak and each surface element can be seen as having its own thermal history disconnected from the other elements. In these conditions, thermal conduction can be modelled as a one-dimensional problem for each individual surface element. Clearly, the body's shape does not play an important role in this formulation. Taking into account only the thermal history of individual surface elements, as outlined above, one may thus succeed in modelling Yarkovsky thermal effects for an ar-

bitrary shape. Of course, when the shape has some symmetry the required algebra becomes much less complicated.

It should be noted that this approach based on individual surface elements was already used by Radzievskii in his pioneering 1952 paper about the thermal force on a spherical body (Radzievskii 1952). Later on, Peterson (1976) adopted a similar formulation when developing a theory for the thermal force on a cylinder and the same was done by Rubincam (1995) in modeling the seasonal Yarkovsky force on a sphere. Vokrouhlický & Farinella (1998) included the nonlinear re-radiation effects by developing a suitable numerical model. However, apart from the papers of Peterson (1976) and Vokrouhlický & Farinella (1998), in all the other studies the body was assumed to be spherical. Thus, relatively little is known about the role of non-sphericity effects in the Yarkovsky force theory.

The aim of this paper is to explore the role of the body's shape on the resulting diurnal Yarkovsky force. In particular, we shall investigate how much the exact results for non-spherical bodies are mismodelled when one adopts a simplified formulation assuming a spherical geometry. Such formulations are common in the studies of the long-term dynamics of the asteroidal fragments (e.g. Afonso et al. 1995; Bottke et al. 1998). In order to assess the validity of the corresponding results, we need to understand the limitations of the thermal models from which the Yarkovsky force is derived.

In order to get a first estimate on the problem, we may use Peterson's (1976) results. Peterson computed the thermal force components (f_X, f_Y) perpendicular to the axis of a cylinder. Rewriting them into the notations introduced in this series of papers we obtain

$$f_X + i f_Y = -\frac{\pi}{3}\, \alpha\, \frac{\mathcal{E}_\star R l}{mc}\, \sin\theta_0\, \frac{(1+\lambda)+i\lambda}{1+2\lambda+2\lambda^2}\ , \tag{1}$$

with

$$\lambda = \frac{\Theta}{4\sqrt{2}}\left(\frac{\pi}{\sin\theta_0}\right)^{3/4}. \tag{2}$$

The parameters and constants are as follows: R is the radius of the cylinder, l its length, m its mass, $\mathcal{E}_\star$ the external radiation flux, c the velocity of light and α the optical absorption coefficient of the surface. The thermal parameter Θ, to be defined below, is used here instead of Peterson's parameter P. We have slightly generalized Peterson's result [Eqs. (17) in his paper], allowing for an arbitrary angle θ_0 between the cylinder's axis and the direction toward the Sun (Peterson assumed $\theta_0 = 90°$). Assuming a value $\gg 1$ for the thermal parameter Θ, we can compare (1) to the corresponding thermal force components for a spherical body (23). Considering a cylinder of radius equal to the radius of the sphere and a length such that the two bodies have equal mass, we obtain that both components from (1) are a factor $2\sqrt{2}(\sin\theta_0/\pi)^{3/4}$ larger than the corresponding components from Eq. (23) below. When $\theta_0 = 90°$, with the solar direction perpendicular to the spin axis of the body, this means that the force acting on a cylinder is about 20 % greater than that on a sphere with the same mass. When θ_0 becomes smaller, the solar direction gets aligned with the cylinder's axis, and both equatorial thermal force components become much smaller than for the comparison sphere.

Is this result representative enough? Is the "equatorial" $\approx 20\%$ error estimate valid for bodies with different shapes? These are the questions which will be addressed in this paper. Of course, we will study a specific class of non-spherical bodies, namely a sequence of axisymmetric ellipsoids (spheroids) with an arbitrary flattening. Both oblate and prolate spheroids will be considered. For the sake of simplicity, we shall first assume (Sect. 2.2) that the rotation axis is aligned with the axis of symmetry. In this particular case, the solution can be obtained in a closed analytical form. However, real asteroidal fragments may survive for relatively long times in a tumbling rotational state, characterized by a misalignment between the rotation axis and the symmetry axis (e.g., Burns & Safronov 1973, Harris 1994, Giblin & Farinella 1997). For this reason, we will also compute the diurnal Yarkovsky force on a body with an arbitrarily oriented spin axis. Due to the algebraic complexity, these latter results will be given numerically. A linear approximation for the grey-body thermal re-emission will be assumed throughout this paper (see Vokrouhlický 1998).

2. Theory

2.1. Spherical bodies

We start our discussion of the diurnal Yarkovsky effect by recalling the results for a spherical body. Although this case was dealt with in paper I, a summary is useful for two different reasons: (i) we intend to introduce the computation method used later on in this paper by illustrating it in the algebraically simpler case of a spherical body, and (ii) the corresponding results will be used for a comparison with the more general results to be derived later. Interestingly, we shall also demonstrate that our method overcomes an intricate and laborious feature of Peterson's (1976) approach, namely the use the Padé approximation for his infinite series (25). By a more direct and simpler computation we will obtain a more precise result, because the Padé approximant method does not yield the required coefficients with a very high precision.

2.1.1. Formulation of the problem

The one-dimensional heat conduction process in a solid medium is described by the parabolic equation

$$\rho C \frac{\partial T}{\partial t} = K \frac{\partial^2 T}{\partial x^2}\ , \tag{3}$$

yielding the distribution of temperature T at depth x and time t. We assume that x increases toward the centre and is 0 on the surface. K is the thermal conductivity, C the specific heat and ρ the density of the material. As in paper I, we shall assume that all these parameters are constant.

The solution of (3) is constrained by a regularity condition at "infinite depth" in the body ($x \to \infty$), and by the energy conservation equation

$$\epsilon \sigma T^4 - K \left(\frac{\partial T}{\partial x} \right)_0 = \alpha \mathcal{E} , \tag{4}$$

at the surface ($x = 0$). We use a grey-body approximation, with an emissivity ϵ for the body's thermal re-radiation of the absorbed energy; α is the absorption coefficient, $\mathcal{E}$ the external radiation flux on the chosen surface element and σ the Stefan-Boltzmann constant. The second term on the left-hand side corresponds to the thermal energy conducted into the body.

The linearization of the emission term in (4) is necessary to obtain a sufficiently simple analytical result. In addition to the assumption about the "large" size of the body discussed above, this linearization provides the second fundamental simplification of our method. Mathematically, it means splitting the temperature T into a properly chosen mean value T_a and a variation ΔT: $T = T_a + \Delta T$.

2.1.2. A suitable choice of variables

Before working out the solution of the problem, a careful choice of variables is necessary. Following previous work in this field (Spencer et al. 1989, Vokrouhlický & Farinella 1998, Vokrouhlický 1998), we adopt the following set of non-dimensional quantities:

- the linear coordinate x will be scaled by the diurnal thermal length l_s given by

$$l_s = \sqrt{\frac{K}{\rho C \omega}} , \tag{5}$$

  where ω is the angular velocity of rotation, and will be denoted by $x' = x/l_s$,
- the time t will be replaced by the complex variable ζ given by

$$\zeta = \exp(i\omega t) \tag{6}$$

  ($i = \sqrt{-1}$ is the imaginary unit);
- the temperature T will be scaled by an auxiliary parameter $T_\star$ defined by

$$\epsilon \sigma T_\star^4 = \alpha \mathcal{E}_\star , \tag{7}$$

  where $\mathcal{E}_\star$ is the solar radiation flux at the distance of the fragment. The resulting non-dimensional variable will be denoted by $T' = T/T_\star$, and similarly $\Delta T' = \Delta T/T_\star$;
- the energy source term $\mathcal{E}$ in the right-hand side of (4) will be scaled by the reference flux $\mathcal{E}_\star$, thus defining $\mathcal{E}' = \mathcal{E}/\mathcal{E}_\star$.

Before formulating the basic equations in the new set of variables, some comments are in order. First, the mean temperature T_a defined previously is not to be confused with the auxiliary value $T_\star$. On the contrary, we shall note below that for a spherical body a natural choice is $T_a' = T_a/T_\star = 1/\sqrt{2}$. Second, a major difference between our method and that of Peterson (1976) is our choice of a single mean temperature for *all* the surface elements on the sphere. Peterson, following the original method of Radzievskii (1952), decided to define the mean temperature separately at each latitude on the sphere. However, we shall demonstrate below that this choice turns out to be algebraically very laborious and unnecessary. Third, the only parameter appearing in our transformed equations will be:

$$\Theta = \frac{\Gamma \sqrt{\omega}}{\epsilon \sigma T_\star^3} , \tag{8}$$

where $\Gamma = \sqrt{\rho C K}$ is the thermal inertia. In agreement with usual terminology we shall call Θ just "thermal parameter". Note that Peterson's parameter P is related to Θ by a numerical factor of order unity (e.g. Vokrouhlický 1998).

Adopting this new set of variables, the heat conduction equation (3) takes the following form

$$i\zeta \frac{\partial}{\partial \zeta} \Delta T'(x'; \theta, \phi; \zeta) = \frac{\partial^2}{\partial x'^2} \Delta T'(x'; \theta, \phi; \zeta) \tag{9}$$

whereas the linearized boundary constraint (4) reads

$$\sqrt{2}\Delta T' - \Theta \left(\frac{\partial \Delta T'}{\partial x'} \right)_0 = \alpha \Delta \mathcal{E}' . \tag{10}$$

The energy-source function $\Delta \mathcal{E}'$ is defined by: $\Delta \mathcal{E}' = \mathcal{E}' - \frac{1}{4}$. The $1/4$ term here compensates for the definition of the mean temperature, $T_a' = 1/\sqrt{2}$.

2.1.3. Radiation source term

Before we derive a solution of the system (9) and (10), we comment on a suitable expansion of the source term $\Delta \mathcal{E}'$. This issue is related to a definition of the reference system to be used hereafter.

Considering a spherical shape of the body, we shall parametrize the individual surface elements by the spherical coordinates θ and ϕ (the colatitude θ is measured from the body's spin axis). The reference system used for the solution of the heat conduction problem is rigidly rotating with the body. Its z-axis is aligned with the spin axis and the equatorial x-axis is chosen so that the direction toward the radiation source (the Sun) lies in the xz-plane at an arbitrary time $t = 0$ (for a diagram see Fig. 1 in Vokrouhlický 1998). Then, the unit position vector of the Sun reads

$$\mathbf{n}_0 = \begin{pmatrix} \frac{1}{2} \sin \theta_0 \zeta \\ \frac{i}{2} \sin \theta_0 \zeta \\ \cos \theta_0 \end{pmatrix} + \text{C.C.} , \tag{11}$$

where θ_0 is the solar colatitude and C.C. stands for a complex conjugate quantity. The scaled solar radiation flux onto a chosen surface element with a position unit vector $\mathbf{n}(\theta, \phi)$ is

$$\begin{aligned} \mathcal{E}' &= \mathbf{n}(\theta, \phi) \cdot \mathbf{n}_0(\theta_0, \zeta) && \text{if } (\mathbf{n} \cdot \mathbf{n}_0) > 0, \\ &= 0 && \text{otherwise.} \end{aligned} \tag{12}$$

This function can be expanded into a Fourier series

$$\mathcal{E}' = \sum_{n \in \mathbf{Z}} \varepsilon_n(\theta, \phi; \theta_0)\, \zeta^n \,, \tag{13}$$

(here $\mathbf{Z}$ denotes the integer numbers), with coefficients given by

$$\varepsilon_n(\theta, \phi; \theta_0) = \frac{1}{2}\, a_n(\theta; \theta_0)\, (\cos n\phi + i \sin n\phi) \,. \tag{14}$$

The first two a functions read

$$a_0(\theta; \theta_0) = \frac{2}{\pi} \left(\phi_\star \cos\theta \cos\theta_0 + \sin\phi_\star \sin\theta \sin\theta_0 \right) \,, \tag{15}$$

$$a_1(\theta; \theta_0) = \frac{1}{\pi} \Big[2 \sin\phi_\star \cos\theta \cos\theta_0$$

$$+ (\phi_\star + \sin\phi_\star \cos\phi_\star) \sin\theta \sin\theta_0 \Big] \,. \tag{16}$$

The auxiliary angle $\phi_\star$ is defined by

$$\begin{aligned}
\cos\phi_\star(\theta, \theta_0) &= -1 & \text{for } \theta < \theta_- \\
&= -\mathrm{ctg}\theta\, \mathrm{ctg}\theta_0 & \text{for } \theta \in (\theta_-, \theta_+) \\
&= 1 & \text{for } \theta > \theta_+
\end{aligned} \tag{17}$$

with $\theta_\pm = \frac{\pi}{2} \pm \theta_0$. Similar expressions can also be found for higher-order terms, but these will not be needed further on.

2.1.4. Regular solution satisfying the boundary constraint

After having discussed the source term, we are ready to find a solution of the problem (9) with the surface constraint (10). First we determine a general form of the solution which is regular throughout the body.

The linearity of the heat conduction equation (7) allows a convenient separation of the variables. We may write

$$\Delta T'(x'; \theta, \phi; \zeta) = \sum_{n \in \mathbf{Z}} t_n(x'; \theta, \phi)\, \zeta^n \,. \tag{18}$$

Substituting this Fourier representation into (9), we obtain a system of decoupled second-order differential equations for the amplitudes t_n. The general solution, which is regular inside the body (i.e. for $x' \to \infty$), reads

$$t_n = c_n \exp\left(-\sqrt{-in}x'\right) \,, \tag{19}$$

with the constants c_n to be determined by the boundary constraint (10). Easy algebra leads to

$$c_0 = \frac{1}{\sqrt{2}} \left(\varepsilon_0 - \frac{1}{4} \right) \tag{20}$$

$$c_n = \frac{\varepsilon_n}{\sqrt{2}} \frac{(1+\lambda_n) - i\lambda_n}{1 + 2\lambda_n + 2\lambda_n^2} \equiv \frac{\varepsilon_n}{\sqrt{2}}\, g_n \exp\left(i\delta_n\right) \tag{21}$$

where $\lambda_n \equiv \Theta\sqrt{n}/2$.

2.1.5. Thermal force and related quantities

Having determined the surface temperature for each of the elements we can now compute the thermal recoil force. We shall assume Lambert's isotropic thermal emission geometry, as before, and linearize the fourth-power emission law. Calling $\mathbf{f}$ the thermal force per unit of the body mass m we obtain

$$\mathbf{f} = -\frac{2\sqrt{2}}{3\pi}\, \alpha\Phi \int d\Omega\, \Delta T'\, \mathbf{n} \,, \tag{22}$$

where $\Phi = (\mathcal{E}_\star \pi R^2)/(mc)$ is the usual radiation force factor. The integration is performed on the whole sphere and $d\Omega = \sin\theta d\theta d\phi$. Finally, the resulting force is expressed into a non-rotating reference frame XYZ, whose Z-axis coincides with the body's spin axis and the X-axis coincides with the x-axis of the rotating frame at time $t = 0$. The force components in this new system read

$$f_X + if_Y = -\frac{4}{9}\, \alpha\, \Phi\, \sin\theta_0\, \frac{(1+\lambda_1) + i\lambda_1}{1 + 2\lambda_1 + 2\lambda_1^2} \,, \tag{23}$$

$$f_Z = -\frac{4}{9}\, \alpha\, \Phi\, \cos\theta_0 \,. \tag{24}$$

This solution can be directly compared with Eqs. (33,34) in Vokrouhlický (1998). As expected, the two solutions coincide in limit of "large bodies" ($R' \to \infty$ in Vokrouhlický 1998). In this approximation the spin-axis aligned component f_Z is simply caused by diffusion of sunlight from the body, without any influence of heat conduction. On the contrary, the equatorial components f_X and f_Y are influenced by heat conduction in the body. Our solution also matches well the solution of Peterson (1976). However, we did not need to compute the involved Padé representation of the final force. As mentioned earlier, the global choice of the mean temperature T_a on the sphere is the main source of this simplification.

2.2. *Spheroidal bodies rotating around their axis of symmetry*

In what follows, we discuss generalization of the previous solution to the case of bodies with a more complex shape. Notably, we consider a class of the spheroids with equatorial radius R and polar radius $(e\,R)$. The parameter e may be both smaller and larger than unity allowing us to treat both oblate and prolate spheroids. We relegate some basic results on the geometry of quadratic surfaces to the Appendix.

2.2.1. Heat conduction problem in a spheroid

Let us first describe the body's rotation. Contrary to the uniform rotation around a fixed axis which can be assumed for a spherical body, the free rotation of an axisymmetric object is more complicated. Generally, it consists of a proper rotation around the axis of symmetry which, in turn, precesses around a constant direction in space. The thermal effects on a body whose axis of symmetry precesses in space will be discussed in Sect. 2.3, and for the moment we shall deal with the simpler case of a uniform rotation around the axis of symmetry. This will allow us

to solve the problem analytically. In fact, most of the previous calculations remain unchanged. We shall just comment on a few differences.

First, we have the definition of the mean temperature T_a. As before, this quantity follows from the balance of the absorbed and re-radiated energy over one rotation cycle of the body

$$- \alpha \mathcal{E}_\star \int_{|\zeta|=1} \frac{id\zeta}{\zeta} P(\theta_0) = S\epsilon\sigma T_a^4 . \tag{25}$$

Here $P(\theta_0)$ is the geometric cross-section of the body when seen from a direction at an angle θ_0 from the axis of symmetry and S is its surface area. Scaling T_a by the reference temperature $T_\star$ we obtain

$$T_a' = \frac{1}{\sqrt{2}} \left[\frac{J_2(\theta_0)}{s(e)} \right]^{1/4} \equiv \frac{1}{\sqrt{2}} \mu(\theta_0; e) , \tag{26}$$

where $s(e)$ is the surface-area scaling function given by the Eq. (A2) in the Appendix, and $J_n(x)$ $(n = 1, 2, 3, \ldots)$ are auxiliary functions:

$$J_n(x) = \sqrt{e^n \sin^2 x + \cos^2 x} . \tag{27}$$

Given the expression (26) for the mean temperature, we note that the linearized boundary constraint (10) for the temperature variation $\Delta T'$ reads

$$\sqrt{2}\mu^3 \Delta T' - \Theta \left(\frac{\partial \Delta T'}{\partial x'} \right)_0 = \alpha \Delta \mathcal{E}' , \tag{28}$$

with the source term $\Delta \mathcal{E}' = \mathcal{E}' - \frac{1}{4}\mu^4$. The Fourier representation (13) of this source term is unchanged, but the coefficients are now given by

$$\varepsilon_n(\theta, \phi; \theta_0) = \frac{1}{2} \frac{a_n(\theta; \theta_0)}{J_4(\theta)} (\cos n\phi + i \sin n\phi) . \tag{29}$$

Notice that we keep parametrization of the surface elements on the surface of the spheroid by the spherical angles: θ (colatitude) and ϕ (longitude). The first two functions $a(\theta; \theta_0)$ of (29) now read

$$a_0(\theta; \theta_0) = \frac{2}{\pi} \left(\phi_\star \cos\theta \cos\theta_0 + e^2 \sin\phi_\star \sin\theta \sin\theta_0 \right) , \tag{30}$$

$$a_1(\theta; \theta_0) = \frac{1}{\pi} \left[2\sin\phi_\star \cos\theta \cos\theta_0 \right.$$
$$\left. + e^2 \left(\phi_\star + \sin\phi_\star \cos\phi_\star \right) \sin\theta \sin\theta_0 \right] . \tag{31}$$

and the auxiliary angle $\phi_\star$ is defined by

$$\begin{aligned} \cos\phi_\star(\theta, \theta_0) &= -1 & \text{for } \theta < \theta_- \\ &= -e^{-2} \operatorname{ctg}\theta \operatorname{ctg}\theta_0 & \text{for } \theta \in (\theta_-, \theta_+) \\ &= 1 & \text{for } \theta > \theta_+ \end{aligned} \tag{32}$$

with $\operatorname{ctg}\theta_\pm = \mp e^2 \operatorname{tg}\theta_0$.

Because the heat conduction equation (9) is independent of the particular geometry of the body, the Fourier expansion (18) with coefficients given by (19) is still valid. The only difference

is that the integration constants c_n now must satisfy (28), which yields

$$c_0 = \frac{1}{\sqrt{2}\mu^3} \left(\varepsilon_0 - \frac{1}{4}\mu^4 \right) \tag{33}$$

$$c_n = \frac{\varepsilon_n}{\sqrt{2}\mu^3} \frac{(1 + \lambda_n) - i\lambda_n}{1 + 2\lambda_n + 2\lambda_n^2} \equiv \frac{\varepsilon_n}{\sqrt{2}\mu^3} g_n \exp(i\delta_n) , \tag{34}$$

with $\lambda_n \equiv \Theta\sqrt{n}/(2\mu^3)$.

2.2.2. Diurnal Yarkovsky force on a spheroid

Given the solution for the surface temperature derived above, we can now compute the total thermal recoil acceleration. Integrating over the surface of the spheroid (with $d\Omega = \sin\theta \, d\theta d\phi$ as before), we have

$$\mathbf{f} = -\frac{2\sqrt{2}}{3\pi} \alpha \Phi e^2 \mu^3 \int d\Omega \frac{J_4(\theta)}{J_2^4(\theta)} \Delta T' \mathbf{n}_\perp , \tag{35}$$

where $\mathbf{n}_\perp$ is a unit normal vector to the surface of the body [see Eq. (A4) of the Appendix]. Interestingly, this two-dimensional integration can be worked out analytically as in the case of a spherical body. The thermal acceleration, projected onto the unit vectors of the non-rotating XYZ system, has components:

$$f_X + if_Y = -\frac{4}{9} \alpha \Phi \sin\theta_0 \frac{(1 + \lambda_1) + i\lambda_1}{1 + 2\lambda_1 + 2\lambda_1^2} \psi_{XY}(e) , \tag{36}$$

$$f_Z = -\frac{4}{9} \alpha \Phi \cos\theta_0 \psi_Z(e) . \tag{37}$$

We recall that

$$\lambda_1 = \frac{\Theta}{2} \left[\frac{s(e)}{J_2(\theta_0)} \right]^{3/4} , \tag{38}$$

and the two functions of e in the right-hand sides of (36) and (37) read

$$\psi_{XY}(e) = \frac{3}{4} \frac{e^2}{\eta^2} \left[\frac{1 + \eta^2}{2\eta} \ln\left(\frac{1 + \eta}{1 - \eta} \right) - 1 \right] , \tag{39}$$

$$\psi_Z(e) = \frac{3}{2\eta^2} \left[1 - \frac{e^2}{2\eta} \ln\left(\frac{1 + \eta}{1 - \eta} \right) \right] . \tag{40}$$

The two functions ψ have been plotted in Fig. 1. The equatorial X and Y force components are reduced by the corresponding ψ_{XY} factors in the case of oblate spheroids and *vice versa*. This result is consistent with the intuitive idea that the normal unit vectors $\mathbf{n}_\perp$ to the polar surface elements of oblate spheroids are more aligned with the Z-axis than the corresponding normal vectors on a sphere. On the contrary, the $\mathbf{n}_\perp$ vectors to the equatorial surface elements lean toward the equatorial plane for prolate spheroids, and therefore contribute to enhancing the equatorial components of the thermal force.

However, when we try to decide whether the thermal force components (36) and (37) are smaller or greater than those on a sphere, we should take into account two more factors:

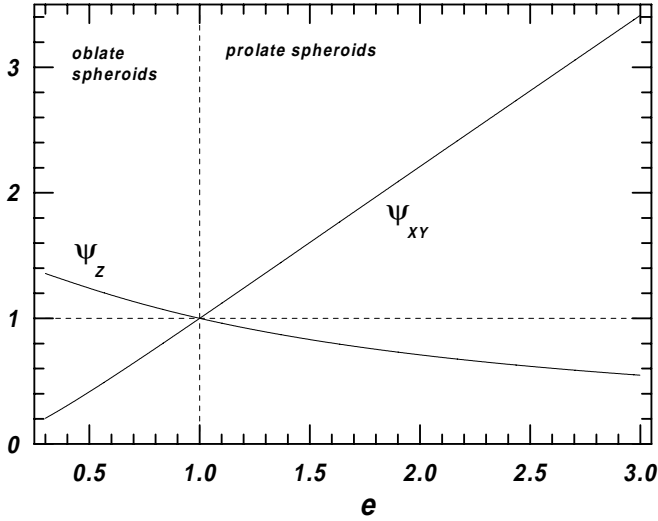– the appearance of the $\mu(\theta_0; e)$ factor in the λ_1 parameter;

Fig. 1. Non-sphericity factors ψ_{XY} and ψ_Z vs. the flattening parameter e.

- the equatorial radius R of the spheroid appearing in the definition of the Φ radiation force factor.

The latter item is related to the problem of the choice of the sphere whose thermal effects should be compared with those for the spheroid. Of course, different such choices are possible. Hereinafter, bodies having the same mass will be compared. Provided the mean density is factorized, equal masses imply that the radius of the comparison sphere has to be $(e^{1/3} R)$. Supposing that the thermal parameter Θ is sufficiently large, we can approximate the rational function of λ_1 in (36) by $\frac{1}{2}(1+i)/\lambda_1$. Then, we conclude that the equatorial thermal force components f_X and f_Y from (36) can be written as the corresponding force components on a sphere (23) multiplied by a numerical factor ξ_{XY}. In a similar way, we define a factor ξ_Z for the third force component f_Z. Putting together the previous results, we have

$$\xi_{XY} \simeq e^{-2/3}\, \psi_{XY}(e)\, \left[\frac{J_2\,(\theta_0)}{s\,(e)}\right]^{3/4} \,, \qquad (41)$$

$$\xi_Z = e^{-2/3}\, \psi_Z(e)\,. \qquad (42)$$

Figs. 2 and 3 show contour plots of the ξ_{XY} factor in the parameter plane θ_0 vs. the flattening parameter e. We note that the maximum differences in the equatorial force components occur for $\theta_0 = 90°$, when the diurnal effect itself is maximum [because of $\sin\theta_0$ factor in Eq. (36)]. The greatest mismodelling (by a factor 2 to 3) is observed when e reaches values as low as 0.3 or as high as 3. The ξ_Z factor has the same dependence on e as the previously discussed function ψ_Z – see Fig. 4.

2.3. Spheroidal bodies rotating around an arbitrary axis

In this section we shall generalize the previous results to the case when the symmetry axis of the spheroid tumbles around a fixed direction in space. Such a free-precessional state seems
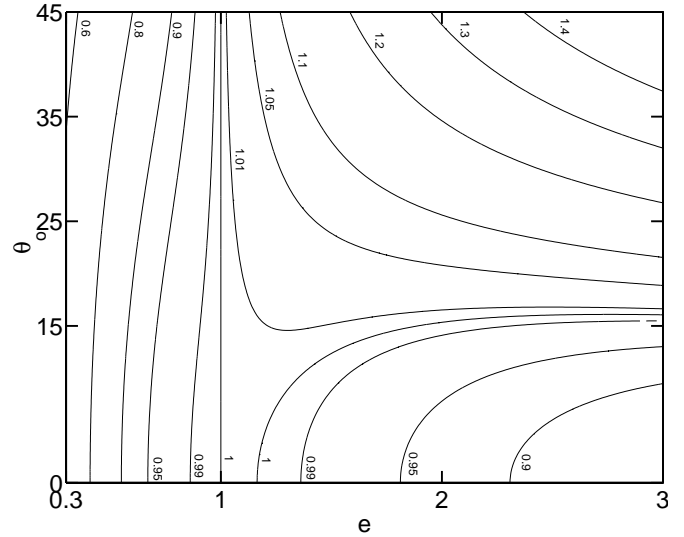

Fig. 2. Curves corresponding to a constant ξ_{XY} factor projected on the plane defined by the solar tilt angle θ_0 (smaller than $45°$) and the body's flattening parameter e. The values of ξ_{XY} label the different curves: $\xi_{XY} > 1$ means that the thermal equatorial components are larger than for a spherical body with the same mass and *vice versa*.
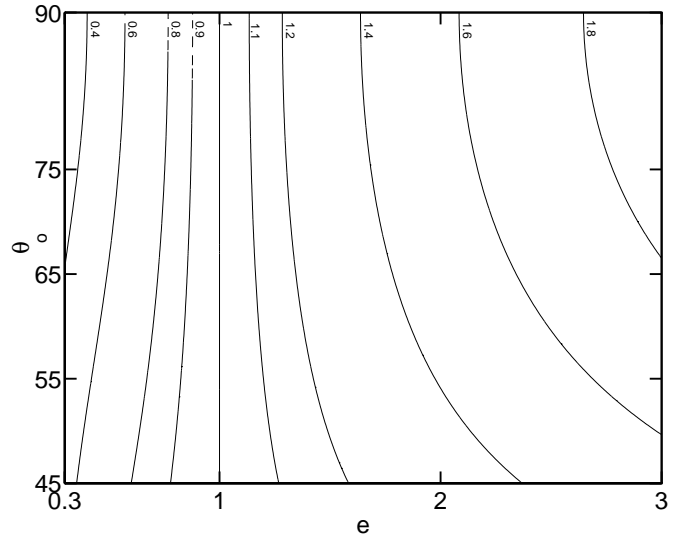

Fig. 3. The same as in Fig. 2 but for θ_0 greater than $45°$.

to be a natural rotational mode for meter-sized asteroidal fragments, since the internal dissipation of energy is not efficient enough to align the spin axis with the angular momentum vector in a short time. According to the theory of Burns & Safronov (1973) the typical time scale for such a dissipation process is about 2 Byr (considering rather conservative values of the dissipation parameter), whereas in the main asteroid belt collisions transferring relatively large amounts of angular momentum typically occur every few Myr only, and for stony bodies shattering impacts occur every few tens of Myr (Farinella et al. 1998). A generalization of the previous results to the tumbling rotation case appears also important for another reason: as the spin axis sweeps the precession cone, different parts of the surface are
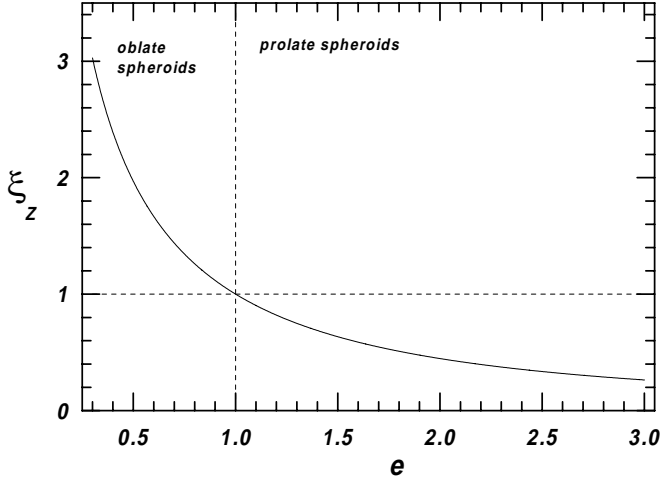
Fig. 4. ξ_Z vs. the flattening parameter e.

more efficiently illuminated by the radiation flux. One might expect that a more uniform distribution of surface temperatures will be established, decreasing the amplitude of the thermal acceleration.

The orientation in space of the reference frame rigidly rotating with the body (whose z-axis coincides with the symmetry axis) will be described by three Euler angles:

– $\psi_E = \omega t$ is the precession angle describing the motion of the projection of the symmetry axis on the XY equatorial plane of the non-rotating reference frame, whose Z-axis coincides with the angular momentum vector;
– $\theta_E = \tau = $ constant is the nutation angle between the symmetry axis (z) and the Z-axis of the non-rotating system;
– φ_E is the angle of proper rotation.

To be consistent with the previous notations, we shall describe the transformation between the two frames by a 3-2-3 sequence of individual rotations, meaning that the second rotation (by the constant nutation angle θ_E) is performed around the y-axis. The Euler angles used in this paper thus differ slightly from the classical set of Euler angles given in the 3-1-3 sequence.

Since the precession frequency is ω, taking $\zeta = \exp(i\omega t)$ as before, the proper rotation velocity is

$$\frac{1}{\omega}\frac{d\varphi_E}{dt} = -\frac{C-A}{C}\cos\tau = -\frac{\eta^2}{2}\cos\tau \tag{43}$$

(see e.g. Landau & Lifschitz 1960), where C and A are the principal moments of inertia around the axis of symmetry and an equatorial axis, respectively, and for homogeneous spheroids we have $(C-A)/C = \frac{1}{2}\eta^2$.

The general scheme outlined in Sect. 2.1 is unchanged, because it concerns the individual thermal histories of different surface elements of the body. What becomes more complicated is mainly the definition of the mean temperature T'_a and the radiation flux term $\Delta\mathcal{E}'$. We shall now discuss these quantities in some detail.

Consider a surface element dS specified by spherical angles θ and ϕ in the system rigidly rotating with the body. The external

radiation flux through this element (scaled by $\mathcal{E}_\star$) is

$$\mathcal{E}'(\theta,\phi;\theta_0,\zeta) = \mathbf{R}_\tau^2\,\mathbf{R}_{\varphi_E(\zeta)}^3\,\mathbf{n}_\perp(\theta,\phi)\cdot\mathbf{n}_0(\theta_0,\zeta)$$
$$\text{if not negative,}$$
$$= 0 \qquad\qquad\quad \text{otherwise,} \tag{44}$$

which generalizes Eq. (12), valid for a spherical body. $\mathbf{R}_\tau^2$ and $\mathbf{R}_{\varphi_E}^3$ are the usual orthonormal rotation matrixes around the $y-$ and z-axes (the angle is specified by the index). The simplicity of the solution for thermal effects from the previous Sects. 2.1 and 2.2 is mainly based on the linearity of the heat conduction equation (9) and the boundary constraints (10) or (28). However, the exact periodicity of the solution, expressed by the Fourier expansions of all the important variables [in particular the temperature T' in Eq. (18)] was an equally important assumption. The ortonormality of the Fourier modes allowed us to decouple the differential equations for the t_n amplitudes of the temperature terms in Eq. (18). This second key property of the diurnal thermal effect solution is violated in the case of a tumbling spin axis, because the precession frequency $\dot\psi_E = \omega$ and the proper rotation frequency $\dot\varphi_E = -\frac{1}{2}\eta^2\cos\tau\,\omega$ - in general are not commensurable with each other.

In order to keep our solution simple enough, we shall adopt a two-step simplifying approach:

– first, we shall neglect the proper rotation of the body, assuming $\frac{1}{2}\eta^2\cos\tau \ll 1$; then the rotation matrix $R_{\varphi_E(\zeta)}^3$ can be approximated by a unit, time independent matrix;
– second, we shall verify the validity of the above-mentioned solution on resonance "slices" defined by $\dot\varphi_E/\dot\psi_E = -\frac{1}{2}\eta^2\cos\tau = -1/n$, where n is an integer number ≥ 1.

In the latter case the periodicity of the diurnal effect solution is that of the proper rotation (n times the precession period). Although we shall not solve the problem in the most general case, we believe that our results are rich enough to give an idea about the role of non-sphericity effects for tumbling fragments.

2.3.1. Proper rotation neglected

In the first step of our approximation we disregard the proper rotation of the body around its symmetry axis. We can then expand the insolation function $\Delta\mathcal{E}'$ of the boundary condition (28) in the Fourier series (13), with coefficients ε_n computed numerically (for $n \neq 0$) by

$$\varepsilon_n(\theta,\phi;\theta_0) = \frac{1}{2\pi i}\int_{|\zeta|=1}\frac{d\zeta}{\zeta^{n+1}}\,\mathcal{E}'(\theta,\phi;\theta_0,\zeta)\,. \tag{45}$$

The ($n=0$) coefficient constrains, like in the previous discussion, the value of the mean temperature $T'_a \equiv \mu(\theta_0;e,\tau)/\sqrt{2}$. The balance between the total energy absorbed by the body over one precessional cycle and the amount of thermally re-radiated energy over the same period is expressed by

$$\int d(\cos\theta)d\phi\,\frac{J_4(\theta)}{J_2^4(\theta)}\,\varepsilon_0(\theta,\phi;\theta_0) = 0\,, \tag{46}$$

with the integration performed over the whole surface of the body and $\varepsilon_0(\theta, \phi; \theta_0)$ given by

$$\varepsilon_0(\theta, \phi; \theta_0) = \frac{1}{2\pi i} \int_{|\zeta|=1} \frac{d\zeta}{\zeta} \left[\mathcal{E}'(\theta, \phi; \theta_0, \zeta) - \frac{1}{4}\mu^4 \right] .$$

(47)

Eqs. (46) and (47) provide the μ factor appearing in the mean temperature in the form

$$\mu(\theta_0; e, \tau) = \left[\frac{\mathcal{I}(\tau, \theta_0; e)}{s(e)} \right]^{1/4} ,$$

(48)

where the integral $\mathcal{I}$ is given by

$$\mathcal{I}(\tau, \theta_0; e) = \frac{e}{\pi} \int_{c_+}^{c_-} dx \sqrt{\frac{1 + \nu x^2}{(x - c_+)(c_- - x)}} .$$

(49)

Here, we denoted $\nu = (1 - e^2)/e^2$ and $c_\pm = \cos(\theta_0 \pm \tau)$. In general, the right-hand side of (49) should be computed numerically, but in some particular cases it is integrable analytically. For later use, we note that in the case of the configuration $\theta_0 = 90°$ (solar direction normal to the rotation axis) we obtain

$$\mathcal{I}(\tau, \pi/2; e) = \frac{2e}{\pi} \sqrt{1 + \nu \sin^2 \tau} \, E\left(\sqrt{\frac{\nu \sin^2 \tau}{1 + \nu \sin^2 \tau}} \right)$$

$$\text{for } e \leq 1 , \quad (50)$$

$$= \frac{2e}{\pi} E\left(\sqrt{-\nu \sin^2 \tau} \right) \quad \text{for } e \geq 1 . \quad (51)$$

Here E is the complete elliptic integral of the second kind. Expressions for $e \leq 1$ and $e \geq 1$ can be obtained from each other by means of the complex argument transformation of elliptic functions:

$$E\left(i\frac{k}{\sqrt{1 - k^2}} \right) = \frac{E(k)}{\sqrt{1 - k^2}}$$

(52)

(see e.g. Byrd & Friedman 1971). Having pre-computed numerically all the previous functions, we can determine the thermal force averaged over one precessional cycle in the non-rotating inertial system. The temperature of each surface element can be expanded in the Fourier series (18), with the amplitude functions given by (19). The surface boundary constraint then yields the integration constants (33) and (34). Finally, the thermal force is obtained by numerical integration of (35) over the whole surface of the spheroid, with the unit normal vector $\mathbf{n}_\perp$ of (A4) transformed into the non-rotating system using the rotation matrix $\mathbf{R}^3_{\psi_E} \mathbf{R}^2_\tau$. After performing all the necessary algebra we obtain

$$f_X = -\frac{2}{3}\alpha \, \Phi \, \frac{e^2}{1 + 2\lambda_1 + 2\lambda_1^2} \times$$

$$\left\{ e^2 \cos \tau \left[(1 + \lambda_1) \mathrm{Re} E_{1,X} + \lambda_1 \mathrm{Im} E_{1,X} \right] \right.$$

$$+ \sin \tau \left[(1 + \lambda_1) \mathrm{Re} E_{1,Z} + \lambda_1 \mathrm{Im} E_{1,Z} \right]$$

$$\left. - e^2 \left[\lambda_1 \mathrm{Re} E_{1,Y} - (1 + \lambda_1) \mathrm{Im} E_{1,Y} \right] \right\} , \quad (53)$$

$$f_Y = -\frac{2}{3}\alpha \, \Phi \, \frac{e^2}{1 + 2\lambda_1 + 2\lambda_1^2} \times$$
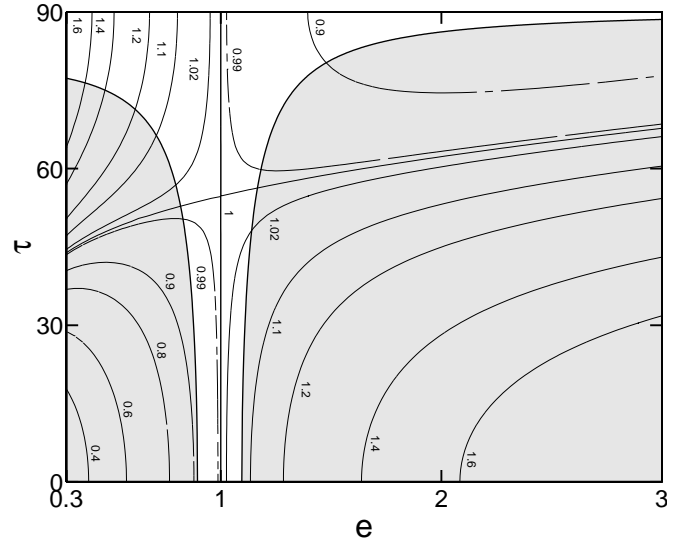
Fig. 5. Contour plot of the ξ_{XY} function in the plane defined by the spin axis tilt τ from the axis of symmetry and the flattening parameter. Each contour line is labelled by the corresponding value of ξ_{XY}. The solar direction is assumed to be normal to the spin axis ($\theta_0 = 90°$). In the shaded area the proper rotation frequency $\dot{\varphi}_E$ is greater than $\frac{1}{10} \dot{\psi}_E$.

$$\left\{ e^2 \cos \tau \left[\lambda_1 \mathrm{Re} E_{1,X} - (1 + \lambda_1) \mathrm{Im} E_{1,X} \right] \right.$$

$$+ \sin \tau \left[\lambda_1 \mathrm{Re} E_{1,Z} - (1 + \lambda_1) \mathrm{Im} E_{1,Z} \right]$$

$$\left. + e^2 \left[(1 + \lambda_1) \mathrm{Re} E_{1,Y} + \lambda_1 \mathrm{Im} E_{1,Y} \right] \right\} , \quad (54)$$

$$f_Z = -\frac{2}{3}\alpha \, \Phi \, e^2 \left(\cos \tau E_{0,Z} - e^2 \sin \tau E_{0,X} \right)$$

(55)

for the three thermal force components. The auxiliary vector quantities $\mathbf{E}_n$ are defined by

$$\mathbf{E}_n(\theta_0) = \int d(\cos \theta) d\phi \, \frac{J_4(\theta)}{J_2^4(\theta)} \, \varepsilon_n(\theta, \phi; \theta_0) \, \mathbf{n}_\perp ,$$

(56)

and the thermal parameter coefficient λ_1 reads

$$\lambda_1 = \frac{\Theta}{2} \left[\frac{s(e)}{\mathcal{I}(\tau, \theta_0; e)} \right]^{3/4} .$$

(57)

Obviously, Eqs. (53) - (55) become equal to (36) and (37) for $\tau = 0$ (so that the symmetry axis of the body coincides with the rotation axis). This property can be easily verified since in this limit $\mathrm{Re}(E_{1,X}) = \mathrm{Im}(E_{1,Y})$ and $\mathrm{Re}(E_{1,Y}) = \mathrm{Im}(E_{1,X})$.

Adopting the methodology of Sect. 2.1 to compare the thermal force components (53) - (55) with the corresponding thermal force acting on a sphere, we define the "correction factors" ξ_{XY} and ξ_Z by: $\xi_{XY} = f_X/f_X^{\mathrm{sphere}} = f_Y/f_Y^{\mathrm{sphere}}$ and $\xi_Z = f_Z/f_Z^{\mathrm{sphere}}$. A sufficiently large value of the thermal parameter Θ is assumed and bodies having the same total mass are compared. Fig. 5 shows contour curves of ξ_{XY} in the plane τ vs. e. As an example, we have assumed the special configuration $\theta_0 = 90°$ in which the thermal equatorial force components are maximum. The results for $\tau = 0$ match those for $\theta_0 = 90°$ in

Fig. 3. A reversal in the magnitude of the equatorial force components compared to those acting on a sphere at large values of τ has to be noted. For small values of τ and oblate spheroids ($e < 1$), for instance, the surface normal vectors $\mathbf{n}_\perp$ in the integral (35) are preferentially directed along the Z-axis, thus decreasing the amplitude of the equatorial force components. The corresponding value of the ξ_{XY} factor is smaller than unity. The opposite occurs for values of $\tau \simeq 90°$ (symmetry axis perpendicular to the rotation axis): in this case the surface normal vectors $\mathbf{n}_\perp$ are preferentially tilted toward the equatorial plane, thus contributing efficiently to the (f_X, f_Y) force components. The corresponding ξ_{XY} factor is larger than unity. Obviously, the situation is just opposite in the case of prolate spheroids ($e > 1$).

The shaded areas in Fig. 5 correspond to the configurations where the ratio between the proper rotation frequency and the precession frequency $\dot{\varphi}_E/\dot{\psi}_E = -\frac{1}{2}\eta^2 \cos\tau$ is larger in absolute magnitude than $\frac{1}{10}$. In this region our simplified solution, neglecting the proper rotation of the body, may not be justified. The large value of the thermal parameter Θ means that the thermal memory time scale is much longer than the rotation period. In this situation, one might expect that the proper rotation could contribute to smearing the surface temperature, decreasing the amplitude of the thermal effects. In the next paragraphs we assess briefly the importance of such phenomena.

2.3.2. The influence of the proper rotation

In the most general case, when the proper rotation angle φ_E is variable, we note that the scaled radiation flux (46) may not be a periodic function. This would violate the basic assumptions of our solution, as discussed above. In order to keep $\mathcal{E}'$ periodic, we shall investigate the thermal effects in the "resonant" cases: $\dot{\varphi}_E/\dot{\psi}_E = -1/n$, where n is an integer. We believe that these cases are representative enough to draw general conclusions.

In the resonant situations the periodicity of $\mathcal{E}'$ and of the whole solution is recovered. The basic time scale is now given by the proper rotation cycle, over which the body undergoes n precessional cycles. All the necessary formulæ for computing the thermal force have been given above. However, as the algebra is rather lengthy, we shall not give here the final results for the thermal force components explicitly.

Fig. 6 shows the ξ_{XY}^n factor vs. the flattening parameter e for three resonance conditions: $n = 2, 5, 10$. The dashed lines are replotted from Fig. 5 to allow a comparison with the case when the proper rotation is neglected, while the solid lines correspond to the complete solution. At the $1:10$ resonance there is a very good agreement between the two results. At the next "slice", corresponding to the $1:5$ resonance, the agreement is still acceptable, whereas in the case of the $1:2$ resonance (precession frequency twice as large as the proper rotation frequency) we observe a significant difference. Interestingly, in the exact solution the force components are larger than the corresponding components from the simplified solution.
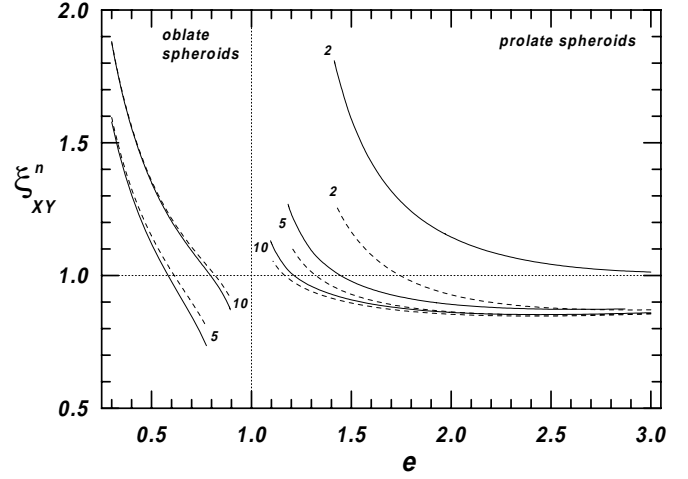

Fig. 6. ξ_{XY}^n vs. the flattening parameter e for some $n : 1$ "resonance slices". The degree n of the resonance labels the curves. The dashed lines correspond to the simple approximation when the proper rotation of the body around its symmetry axis is neglected (results from Fig. 5), while the solid lines account for the proper rotation.
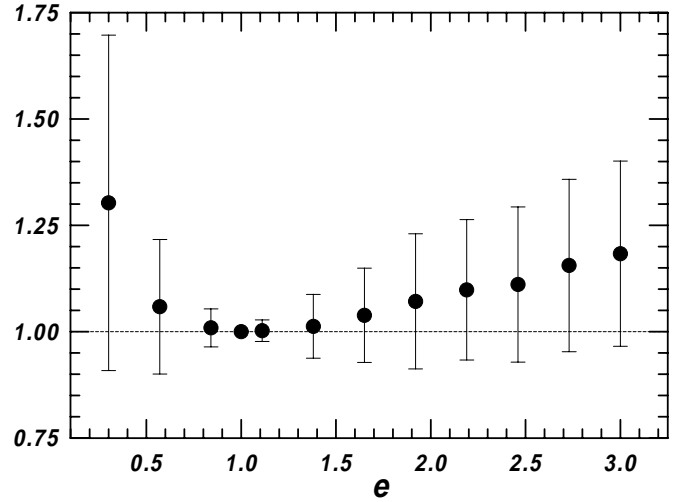

Fig. 7. Mean value of the ξ_{XY}-factor over a random sampling of the nutation angle τ and the solar tilt angle θ_0 (500 values considered), as a function of the flattening parameter e. The proper rotation of the body is neglected. Error bars correspond to the Gaussian standard deviation.

2.3.3. Results averaged over the orientation of the spin axis in space

In the previous discussion we have compared the exact solution for the diurnal Yarkovsky force on spheroids with the corresponding solution for a sphere using a special configuration, that is to say, we had fixed a particular value of the θ_0 angle between the solar direction and the body's spin axis and/or of the τ angle between the symmetry and the spin axes. In reality, these geometric parameters change owing to the body's revolution around the radiation source (the Sun) and the collisions with other asteroid fragments. In both cases the corresponding

time scale is typically much shorter than the period over which the orbital evolution is studied by numerical integrations. Therefore, we might be interested in averaging the ξ_{XY} factor over all the possible configurations of the (θ_0 and τ) angles. The mean values of the ξ_{XY} factor over a sample of 500 random values of the angles together with the corresponding Gaussian standard deviations are shown in Fig. 7. In contrast to the previous results, we get a much better agreement between the diurnal Yarkovsky force computed for spheroids and for a sphere. The peak differences are of the order of 30%, but in most cases are smaller than 20%. As expected, the dispersion of the results – indicated by the standard deviations – is larger for more elongated bodies.

3. Conclusions

The main results of this paper may be summarized as follows:

– The diurnal Yarkovsky recoil force has been computed for bodies whose shape lacks a spherical symmetry, that is for axisymmetrical spheroids with an arbitrary flattening. The only important simplifying assumption of our approach is that the average size of the body must be much larger than the penetration depth of the thermal diurnal wave. The latter spans millimeter to centimeter interval in the typical astonomical applications (basalt meteoroids, lunar rocks, regolith-covered fragments of the asteroids, etc.).
– The results are derived in a closed analytical form if the body rotates around its axis of symmetry. In the more general case of a free-precessing object, the results are given numerically.
– Our main goal has been that of comparing the diurnal Yarkovsky force acting on an irregularly shaped body with that acting on a sphere, since this shape corresponds to a commonly used approximation in the long-term numerical integration schemes for asteroidal fragment orbits. Our results can be used to assess the corresponding mismodelling of the Yarkovsky perturbations found from these integrations.
– Our results indicate that, depending on the geometric parameters (degree of flattening, nutation angle etc.), the simple spherical-shape approximation for the diurnal Yarkovsky force provides results mismodelled up to a factor of 2 or 3.
– However, when an average over all possible pole orientations of a tumbling body and all possible solar direction during its revolution around the Sun is performed, there is a much better agreement between the thermal force acting on a sphere and our results for spheroids. This suggests that neglecting the influence of non-sphericity effects may not degrade significantly the results of long-term orbital integrations including the diurnal Yarkovsky effect.

Of course, there is the possibility that the resulting thermal force may be significantly different for bodies of much more irregular shape than those studied in this paper. This issue is beyond the scopes of the current study and may be require further work in the future. However, it seems very likely that the results will not differ too much in the most general case of a tumbling spin axis, as discussed above.

The analysis of this paper suggests that non-sphericity effects should not be seen as a very serious concern in modelling the diurnal Yarkovsky perturbations. Therefore, in a forthcoming paper we plan to apply the thermal model for the diurnal Yarkovsky effect on a sphere as derived in paper I to a long-term integration of fragment orbits. Several important issues related to the delivery of meteorites and asteroidal fragments to the inner Solar System will be considered.

Appendix A: basics of spheroidal geometry

In the appendix we summarize some basic geometrical relations needed in the main text. We consider an ellipsoid of rotation (called a spheroid above) with equatorial radius R and polar radius (eR). The parameter e represents the geometric flattening of the body: $e \in (0, 1)$ for oblate spheroids and $e > 1$ for prolate spheroids. We need not introduce ellipsoidal coordinates. Rather, we keep the parametrization of the surface elements by the colatitude θ (measured from the axis of symmetry) and the longitude angle ϕ (measured in the equatorial plane from an arbitrary origin). The surface element dS on the spheroid is given by

$$dS = e^2 R^2 \frac{J_4(\theta)}{J_2^4(\theta)} \sin\theta d\theta d\phi \,, \tag{A1}$$

with the auxiliary functions $J_n(\theta)$ given by Eq. (27) above.

The total surface area of the spheroid is then given by $S = 4\pi R^2 \, s(e)$, where

$$s(e) = \frac{1}{2} \left[1 + \frac{e^2}{2\eta} \ln \left(\frac{1+\eta}{1-\eta} \right) \right] \,. \tag{A2}$$

Here, we defined $\eta = \sqrt{1 - e^2}$. Note that in the case of prolate spheroids ($e > 1$), η becomes imaginary; in this case we can use the following identity, holding for any complex number z:

$$\frac{1}{2} \ln[(1+z)/(1-z)] = \frac{1}{i} \mathrm{arctg}(iz) \,. \tag{A3}$$

A unit vector normal to the surface element at colatitude θ and longitude ϕ can be written as

$$\mathbf{n}_\perp(\theta, \phi) = \frac{1}{J_4(\theta)} \begin{pmatrix} e^2 \sin\theta \cos\phi \\ e^2 \sin\theta \sin\phi \\ \cos\theta \end{pmatrix} \,. \tag{A4}$$

Finally, the geometric cross-section P of the spheroid when seen from a direction at an angle θ_0 from the axis of symmetry. Simple algebra yields

$$P(\theta_0) = \pi R^2 \, J_2(\theta_0) \,. \tag{A5}$$

References

Afonso G., R.S. Gomes, M.A. Florczak, 1995, Planet. Space Sci. 43, 787

Binzel R.P., P. Farinella, V. Zappalá, A. Cellino, 1989, in: Asteroids II, eds. R.P. Binzel, T. Gehrels and M.S. Matthews, Univ. of Arizona Press, Tucson, p. 416

Bottke W.F., D.P. Rubincam, J.A. Burns, Consequences of the Yarkovsky effect on the orbital evolution of meteoroids: A prospectus, paper presented at Lunar Planet. Sci. Conf., Houston, 1998

Burns J.A., V.S. Safronov, 1973, MNRAS 165, 403

Byrd P.F., M.D. Friedman, 1971, Handbook of Elliptic Integrals for Engineers and Scientists, Springer-Verlag, Berlin

Catullo V., V. Zappalá, P. Farinella, P. Paolicchi, 1984, AA 138, 464

Farinella P., D. Vokrouhlický, W.K. Hartmann, 1998, Icarus 132, 378

Fujiwara A., G. Kamimoto, A. Tsukamoto, 1978, Nature 272, 602

Fujiwara A., P. Cerroni, D.R. Davis, et al., 1989, in: Asteroids II, eds. R.P. Binzel, T. Gehrels and M.S. Matthews, Univ. Arizona of Press, Tucson, p. 240

Giblin I., G. Martelli, P.N. Smith et al., 1994, Icarus 110, 203

Giblin I., P. Farinella, 1997, Icarus 127, 424

Harris A.W., 1994, Icarus 107, 209

Hartmann W.K., P. Farinella, D. Vokrouhlický, S.J. Weidenschilling, A. Morbidelli, F. Marzari, D.R. Davis, E. Ryan, 1998, Meteoritics Planet. Science, in press

Landau L.D., E.M. Lifschitz, 1960, Mechanics, Addison-Wesley, Reading

Ostro S.J., K.D. Rosema, R.S. Hudson, et al., 1995, Nature 375, 474

Peterson C., 1976, Icarus 29, 91

Radzievskii V.V., 1952, Astron. Zh. 29, 162 (in Russian)

Rubincam D.P., 1995, J. Geophys. Res. 100, 1585

Rubincam D.P., 1998, J. Geophys. Res. 103, 1725

Spencer J.R., L.A. Lebofsky, M.V. Sykes, 1989, Icarus 78, 337

Vokrouhlický D., 1998, AA 335, 1093 (paper I)

Vokrouhlický D., P. Farinella, 1998, Astron. J., in press

Zappalá V., P. Farinella, 1997, Adv. Space Res. 19, 181